NeuroImage 49 (2010) 94–103

Contents lists available at ScienceDirect

NeuroImage

journal homepage: www.elsevier.com/locate/ynimg

Longitudinal changes in grey and white matter during adolescence

A. Giorgio [a,b], K.E. Watkins [a,c], M. Chadwick [a], S. James [d], L. Winmill [d], G. Douaud [a], N. De Stefano [b], P.M. Matthews [a,f,g], S.M. Smith [a], H. Johansen-Berg [a], A.C. James [d,e,*]

[a] Centre for Functional MRI of the Brain, University of Oxford, Oxford, UK
[b] Neurology and Neurometabolic Unit, Department of Neurological and Behavioural Sciences, University of Siena, Italy
[c] Department of Experimental Psychology, University of Oxford, Oxford, UK
[d] Highfield Adolescent Unit, Warneford Hospital, Oxford, UK
[e] Department of Psychiatry, University of Oxford, Oxford, UK
[f] GSK Clinical Imaging Centre, Hammersmith Hospital, London, UK
[g] Department of Clinical Neurosciences, Imperial College, London, UK

ARTICLE INFO

Article history:
Received 10 February 2009
Revised 13 June 2009
Accepted 4 August 2009
Available online 11 August 2009

ABSTRACT

Brain development continues actively during adolescence. Previous MRI studies have shown complex patterns of apparent loss of grey matter (GM) volume and increases in white matter (WM) volume and fractional anisotropy (FA), an index of WM microstructure. In this longitudinal study (mean follow-up = 2.5 ± 0.5 years) of 24 adolescents, we used a voxel-based morphometry (VBM)-style analysis with conventional T1-weighted images to test for age-related changes in GM and WM volumes. We also performed tract-based spatial statistics (TBSS) analysis of diffusion tensor imaging (DTI) data to test for age-related WM changes across the whole brain. Probabilistic tractography was used to carry out quantitative comparisons across subjects in measures of WM microstructure in two fiber tracts important for supporting speech and motor functions (arcuate fasciculus [AF] and corticospinal tract [CST]). The whole-brain analyses identified age-related increases in WM volume and FA bilaterally in many fiber tracts, including AF and many parts of the CST. FA changes were mainly driven by increases in parallel diffusivity, probably reflecting increases in the diameter of the axons forming the fiber tracts. FA values of both left and right AF (but not of the CST) were significantly higher at the end of the follow-up than at baseline. Over the same period, widespread reductions in the cortical GM volume were found. These findings provide imaging-based anatomical data suggesting that brain maturation in adolescence is associated with structural changes enhancing long-distance connectivities in different WM tracts, specifically in the AF and CST, at the same time that cortical GM exhibits synaptic "pruning".

Introduction

Adolescence is defined as the developmental period of transition from childhood to adulthood and is characterized by maturation of cognitive abilities and complex behavioral features (Spear, 2000). Major advances in learning through education are made during adolescence and obvious physical, hormonal, emotional, and social changes occur. By contrast, changes in brain structure during adolescence are more subtle. In the grey matter (GM), these changes take the form of increased myelination of cortico-cortical connections (Nielsen, 1963; Yakovlev and Lecours, 1967) or synaptic "pruning" (Huttenlocher, 1979) or both. Increases in the diameter and myelination of the axons forming the fiber tracts, alongside increased neuronal size and glia proliferation, contribute to the monotonic increase in white matter (WM) volume or density during childhood and adolescence revealed by analysis of magnetic resonance imaging (MRI) scans (Giedd et al., 1999; Paus et al., 1999). Understanding changes in brain structures and the relationship between changes in GM and WM structures during adolescence is an important goal not only to understand normal brain development but also to aid in the study of abnormal neurodevelopment in disorders such as schizophrenia and bipolar disorder (Giedd, 2004; Paus et al., 2008).

Over the past decade, the availability of automated computational techniques for analyzing structural MRI data of the brain has led to a plethora of studies documenting changes during normal childhood and adolescence. These studies are in general agreement that GM volume decreases and WM volume increases during this age range (Barnea-Goraly et al., 2005; Giorgio et al., 2008; Lebel et al., 2008; Paus et al., 1999; Reiss et al., 1996). The literature on changes in WM microstructure, measured using diffusion tensor imaging (DTI), shows a consistent pattern of increased fractional anisotropy (FA) across childhood and adolescence (Ashtari et al., 2007; Barnea-Goraly et al., 2005; Bonekamp et al., 2006; Eluvathingal et al., 2007; Giorgio et

* Corresponding author. Department of Psychiatry, University of Oxford, Warneford Hospital, OX3 7JX Oxford, UK.
E-mail address: anthony.james@psych.ox.ac.uk (A.C. James).

1053-8119/$ – see front matter © 2009 Elsevier Inc. All rights reserved.
doi:10.1016/j.neuroimage.2009.08.003

al., 2008; Lebel et al., 2008; Muetzel et al., 2008; Nagy et al., 2004; Schmithorst et al., 2002). However, previous DTI studies have been cross-sectional, and few have focused on the late adolescent period. Inconsistent findings reflect the need for more targeted studies and highlight the importance of longitudinal studies to enable the reconstruction of the dynamic course and anatomical sequence of the developing brain (Toga et al., 2006).

In general, FA is a quantitative measure of WM organization and structural integrity, but the specific nature of the developmental changes that contribute to the observed changes is unknown. Some fundamental phenomena that could illuminate this also remain to be elucidated. For example, it is unclear whether increases in FA are due to greater diffusivity along the main diffusion axis (Ashtari et al., 2007) or reduced diffusivity along the axes perpendicular to it (Bhagat and Beaulieu, 2004; Bonekamp et al., 2006; Eluvathingal et al., 2007; Giorgio et al., 2008; Snook et al., 2005; Suzuki et al., 2003) or a combination of the two.

Here, we present an analysis of longitudinal data obtained during late adolescence. We analyzed T1-weighted brain images to examine changes in GM and WM volumes and diffusion images to examine changes in WM microstructure. The aims of this study were to (i) replicate and extend previous findings from cross-sectional studies, (ii) explore changes in GM and WM volumes by using a more sensitive longitudinal design, and (iii) examine the nature of the changes in WM microstructure.

To our knowledge, this is the first study to examine within-subject longitudinal changes in diffusion data in healthy adolescents. It also combines analyses of different data types obtained in the same individuals. In fact, we used two whole-brain approaches to measure changes in brain structure: a voxel-based morphometry (VBM)-style analysis to measure changes in GM and WM volumes (Good et al., 2001) and tract-based spatial statistics (TBSS (Smith et al., 2006)) to examine changes in diffusion data. We paid particular attention to diffusion changes in two specific WM pathways, the arcuate fasciculus (AF) and the corticospinal tract (CST). These two pathways had previously been shown to have an increase in WM density in a large cross-sectional study of 4- to 19-year-old subjects (Paus et al., 1999).

Materials and methods

MRI data were acquired at two time points in a group of 24 healthy adolescents (10 males, 14 females; 21 right-handed, 3 left-handed). The median age at baseline was 15.3 years, range was 13.5–18.8 years, and mean was 15.7 ± 1.4 years. This group was selected because the age spread was fairly evenly distributed. All subjects were likely to be in a similar phase of brain reorganization, although, with differing ages, subjects would be at different points along any developmental trajectory. Participants were scanned again after a mean of 2.5 ± 0.56 years; the median age at follow-up was 17.8 years, range was 16.2–22.1 years, and mean was 18.2 ± 1.6 years.

None of the participants had a history of psychiatric or neurological disease or substance misuse. IQ scores were measured by a trained psychology assistant using the Wechsler Abbreviated Scale of Intelligence (WASI) (Wechsler, 1999). The subjects were of normal intelligence (mean IQ score $= 109.4 \pm 12.9$). Informed written consent was obtained from all participants in accordance with ethical approval from the Central Office for Research Ethics Committees (REF no.06/Q1607/67).

Data acquisition

Scans were obtained on a 1.5-T Siemens Sonata MR scanner using a standard single-channel head coil with a maximum gradient strength of 40 mT m^{-1}. For the DTI data, two sets of echo-planar images (EPI) of the whole head were acquired (TR = 8500 ms; TE = 80 ms; 53×2.5 mm axial slices; in-plane resolution 2.5×2.5 mm^2). Each set comprised three non-diffusion-weighted and 60 diffusion-weighted images acquired with a *b*-value of 1000 s mm^{-2} uniformly distributed across 60 gradient directions. A T1-weighted image was also acquired in each participant for a VBM-style analysis and image registration (3D FLASH; TR = 12 ms; TE = 5.6 ms; 1 mm isotropic voxels; matrix $= 256 \times 256 \times 208$; elliptical sampling; orientation = coronal; three averages).

Data analysis

Voxel-based morphometry-style analysis

We employed an 'optimized' VBM-style protocol (Good et al., 2001) using FSL (FMRIB Software Library v4.1, www.fmrib.ox.ac.uk/fsl (Smith et al., 2004)) tools for brain extraction (Smith, 2002) and tissue segmentation (Zhang et al., 2001). FMRIB's Nonlinear Registration Tool (FNIRT) (Andersson et al., 2007a, 2007b) was used to spatially register the native images to a standard-space template. The optimized protocol used to assess linear correlations between regional changes in GM and WM volumes and increase in age was as follows. The raw T1-weighted images were first segmented to form images representing partial volume estimates of each tissue class (Zhang et al., 2001). For the analysis of GM, the 48 GM images were nonlinearly registered to the ICBM-152 GM template, mirror images were created flipping the images across the midline, and a left–right symmetric study-specific GM template was created from the average of these 96 images. The 48 native GM images were then nonlinearly transformed to this template using FNIRT. The signal in each voxel of the transformed images was modulated by the Jacobian determinant of the nonlinear component of the warp field. This modulation adjusts the signal in each voxel to reflect (or compensate for) the amount of contraction or enlargement due to the nonlinear component of the spatial transformation. It should be noted that we chose to exclude the affine component of the registration from the modulation process, therefore adjusting for the linear increase or decrease of global brain size over time. Therefore, significant longitudinal local changes in GM volume should be interpreted as a *relative accelerated* change compared to the effect of age on *global* brain size.

All 48 modulated normalized GM volume images were smoothed with an isotropic Gaussian kernel with a sigma of 3.5 mm (~8 mm FWHM). To test for local correlations between changes in GM volume and increase in age from baseline to follow-up, a paired *t*-test between each subject's images was performed using the difference between age at baseline and follow-up as the covariate of interest. This was implemented using a design matrix containing regressors for each subject's image pair, to remove the subject effect, and a final regressor of age at scan (ages at baseline and follow-up separately), which was orthogonalized to the subject regressors. In other words, this analysis compares the change in GM volume between baseline and follow-up with the increase in age between these two time points. Inference on these statistics was carried out using the "randomize" program within FSL, which performs permutation testing (5000 permutations) (Nichols and Holmes, 2002). Thresholding was carried out using TFCE (Threshold-Free Cluster Enhancement), a new method for finding significant clusters in MRI data without having to define them as binary units (Smith and Nichols, 2009). Clusters were assessed for significance at $p<0.05$, fully corrected for multiple comparisons across space. Anatomical locations of the significant GM clusters were determined by reference to the Harvard-Oxford cortical structural atlas integrated into FSLView (part of FSL).

For the WM, we used a protocol similar to that of the GM (see above). All 48 modulated normalized WM volume images were smoothed with an isotropic Gaussian kernel with a sigma of 4 mm (~10 mm FWHM). The levels of smoothing were chosen to be compatible with previous analysis of similar data (e.g., Giorgio et al., 2008; Paus et al., 1999).

An independent GM and WM VBM-style analysis was carried out in all right-handed subjects, after excluding the three left-handed subjects.

Differences in GM and WM volumes between males and females and the interaction between sex and age were also tested using randomize within VBM-style analysis, with a significance level of $p<0.05$, fully corrected for multiple comparisons across space.

Diffusion data analysis

Diffusion MRI data were pre-processed using DTIFit within the FMRIB Diffusion Toolbox (FDT, part of FSL). Images were corrected for eddy currents and head motion by using affine registration to the nondiffusion volumes ($b=0$). Data were averaged across the two acquisitions to improve signal-to-noise ratio. Images of fractional anisotropy (FA), diffusivity parallel (λ_1), and perpendicular ($(\lambda_2+\lambda_3)/2$) to the principal diffusion direction were obtained. Voxel-wise correlations between within-subject FA changes and subject-specific age increase were assessed using TBSS (also part of FSL (Smith et al., 2006)). FA images were first nonlinearly registered to a target image identified using FNIRT and then averaged. Because the study subjects were all adolescents, the target image was automatically chosen to be the most "typical" or "representative" subject in the study. The average of all the data was thinned to create a "skeleton" of WM, representing the tracts common to all subjects. This WM tract skeleton was thresholded at FA>0.2, resulting in a skeleton with 120767 $1\times1\times1$ mm^3 WM voxels, corresponding to approximately half of the WM voxels of the whole skeleton. TBSS then projects each subject's FA data onto the mean WM tract skeleton. The highest FA value near the skeleton in each subject (which should correspond to the local tract center value) is then projected onto the mean WM tract skeleton for analysis. The FA data were analyzed using the same model as for the GM and WM volume analysis described above in order to examine the linear correlation between changes in FA and increasing age. Statistical inference was carried out using TFCE thresholding in random (5000 permutations). Changes were considered significant at $p<0.05$, which is fully corrected for multiple comparisons across space. An independent TBSS analysis was carried out in all right-handed subjects, after excluding the three left-handed subjects. Using TBSS, differences in FA between males and females and the interaction between sex and age were also tested.

The anatomical location of the significant clusters was determined by reference to a fiber tract-based atlas of human WM anatomy (Wakana et al., 2004) integrated into FSLView. In addition to the FA data used for analysis on the WM skeleton in each participant (see above), the parallel and perpendicular diffusivity data from the same voxels also were processed using the TBSS protocol.

For clusters showing significant correlation between FA and age over time with TBSS, we calculated mean FA, parallel and perpendicular diffusivity values across all voxels within these clusters and plotted these against age to help visualize in each subject the slope of FA, parallel and perpendicular diffusivity values between baseline and follow-up.

In a separate analysis, we used probabilistic tractography (Behrens et al., 2003) to isolate the AF and CST in each hemisphere of each subject at both time points. Tractography was constrained using a multiple region-of-interest (ROI) approach. The ROIs were defined in a common standard space (MNI152 standard template). A combination of four types of masks to constrain the tractography analysis was used: seed mask (all voxels from which probabilistic tractography proceeded), target mask (only those pathways reaching it were retained), termination mask (ROIs "before" seed and "after" target masks, used to terminate pathways beyond these regions), exclusion mask (ROIs used to remove rather than just terminate any pathways entering this region). Tracts that did not pass through the seed and target masks were automatically discarded from the calculation of the connectivity distribution.

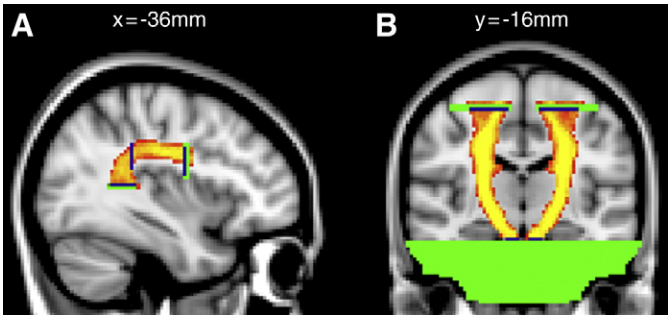

Fig. 1. In red–yellow group pathways thresholded at 20% (i.e., at any given voxel, at least 20% of the subjects had the tract present) for (A) left arcuate fasciculus (AF) and (B) corticospinal tracts (CST). In both images, blue bars represent seed and target masks, green represents termination and exclusion masks. See Materials and methods for details. Background image is the MNI152. Images are shown in radiological convention.

The following symmetrical standard-space masks were defined in each hemisphere and registered to the native diffusion space of each subject using FMRIB Linear Image Registration Tool (FLIRT (Jenkinson and Smith, 2001)).

Arcuate fasciculus masks (Fig. 1A)

1. Seed mask: this comprised voxels located in the WM of the AF just anterior to the point where the tract begins to arc toward a ventral orientation, in a single coronal slice located at $Y=-38$, extending from $X=30$ to 42, and $Z=20$ to 34.
2. Two target masks: the first comprised voxels located in the WM anterior to the seed mask at the level of a single coronal slice at $Y=-6$, extending from $X=26$ to 42, and $Z=16$ to 32. The second comprised voxels ventral to the seed mask, in a single axial slice at $Z=10$, extending from $X=32$ to 44, and $Y=-36$ to -50.
3. Two termination masks: these comprised voxels located just anterior and just below the first and second target masks, respectively.
4. Two exclusion masks: used to remove branches extending outside the AF. The first mask comprised voxels in a single sagittal slice at $X=50$, extending from $Y=-10$ to -62, and $Z=6$ to 44. The second one comprised voxels in a single sagittal slice at $X=22$, extending from $Y=-20$ to 4, and $Z=-4$ to 20.

In order to better isolate the AF, pathways generated in each subject were thresholded to include only voxels in which at least 500 samples (out of 5000 generated from each seed and target voxel at the same time) passed through.

Corticospinal tract masks (Fig. 1B)

1. Seed mask: this comprised the voxels of the whole cerebral peduncle on a single axial slice at the level of $Z=-22$.
2. Target mask: this comprised the voxels located on a single axial slice at the level of $Z=56$, extending from $Y=-12$ to -32 and from $X=10$ to 32.
3. Two termination masks: the first one comprised voxels from the whole brain inferior to $Z=-24$ to terminate fibers traveling below the peduncle. The second one comprised voxels surrounding the target mask at the same axial slice, extending from $X=8$ to 44 and from $Y=-34$ to -4 and including voxels in an area of the same size at one slice above the target mask, at the level of $Z=58$. The latter was used to cut off pathways extending beyond the target mask.

In order to remove spurious connections, pathways generated in each subject were thresholded to include only voxels in which at least

20 samples (out of 5000 generated from each seed and target voxel at the same time) passed through.

This thresholding step refers to the outputs of probabilistic tractography. The final output of tractography is an image in which voxel values across the whole brain represent the number of these pathways passing through that voxel. The number of samples passing through a voxel is interpreted as the probability of that voxel being connected to the seed mask. There is no straightforward statistical framework in which to perform thresholding and so, typically, an arbitrary cutoff is chosen. Here, we chose a value of 20 for the CST and 500 for the AF. Thresholds vary between AF and CST pathways due to the different size of the seed masks and different tracking conditions for each tract. Thresholds were chosen based on pilot data in healthy subjects in order to produce consistent and reproducible tracking results.

Once identified, pathways were binarize. Both FA values and tract volumes were calculated from the binarized masks for these tracts for each hemisphere, subject, and scan. We averaged the binary representations of each tract across subjects to produce probability maps for the AF and CST in each hemisphere separately (Fig. 1).

A repeated-measures analysis of variance (ANOVA) was used to test the effects of time (baseline versus follow-up) and hemisphere on FA and volume values in AF and CST. Comparisons of FA and volume values in AF and CST between baseline and follow-up scans and between left and right cerebral hemispheres in each time point were carried out by paired-samples *t*-tests. These analyses were also performed with interscan interval, which was different across subjects, as a covariate. The relationship between FA and volume of left and right AF and CST at both time points was tested by Pearson's correlation coefficient.

Data were considered significant at two-tailed $p<0.05$. SPSS v16.0 (SPSS Inc., Chicago, Illinois) was used to perform statistical calculations.

Results

Correlations between changes in grey matter volume and age over time

A significant (corrected $p<0.05$) decrease in GM volume with increasing age was found in five clusters (Fig. 2). The largest one encompassed many cortical areas extending from the medial parieto-occipital cortex to bilateral superior and inferior lateral parietal areas including the parietal opercular cortex. In the right hemisphere, this cluster also encompassed central opercular and superior temporal cortex extending to portions of the inferior occipitotemporal cortex and the right cerebellar hemisphere. A smaller additional cluster was found in the left cerebellar hemisphere. Another cluster extended from the medial frontal cortex to the superior frontal gyri bilaterally and further on the right to include the middle and inferior frontal gyri. Two small clusters were located in the left anterior insular cortex and in the left central operculum/planum polare just lateral to Heschl's gyrus. Because of the extent of the largest cluster, which encompassed so many anatomical areas, we lowered the corrected *p*-value threshold to <0.005 to reveal a number of smaller, more anatomically specific and highly significant clusters (Figs. 3A–E and Table 1). No changes in subcortical grey matter were found.

In a separate analysis, we showed that the pattern of these observations was similar by excluding the three left-handed subjects (data not shown).

No significant longitudinal increases in GM volume from baseline to follow-up were found. Males and females showed no significant voxel-wise difference in the degree of age-related change in GM volume.

Correlations between changes in white matter volume and age over time

Significant (corrected $p<0.05$) increases in WM volume from baseline to follow-up with increasing age were found in three clusters (Fig. 2). One cluster was located in the frontal WM bilaterally and was connected via the body of the corpus callosum (CC). The other two clusters symmetrically extended from the retrosplenial WM into the WM underlying the medial parietal cortex and inferiorly into the temporal lobe portion of the cingulum. Furthermore, the cluster on the left also extended posteriorly into the WM underlying occipital cortex and laterally to the left inferior longitudinal fasciculus (ILF). As above, to identify more anatomically specific clusters, we re-thresholded the data at corrected $p<0.005$ (Figs. 3F–L and Table 2).

The same pattern of changes in WM volume with age was seen after excluding the three left-handed subjects (data not shown).

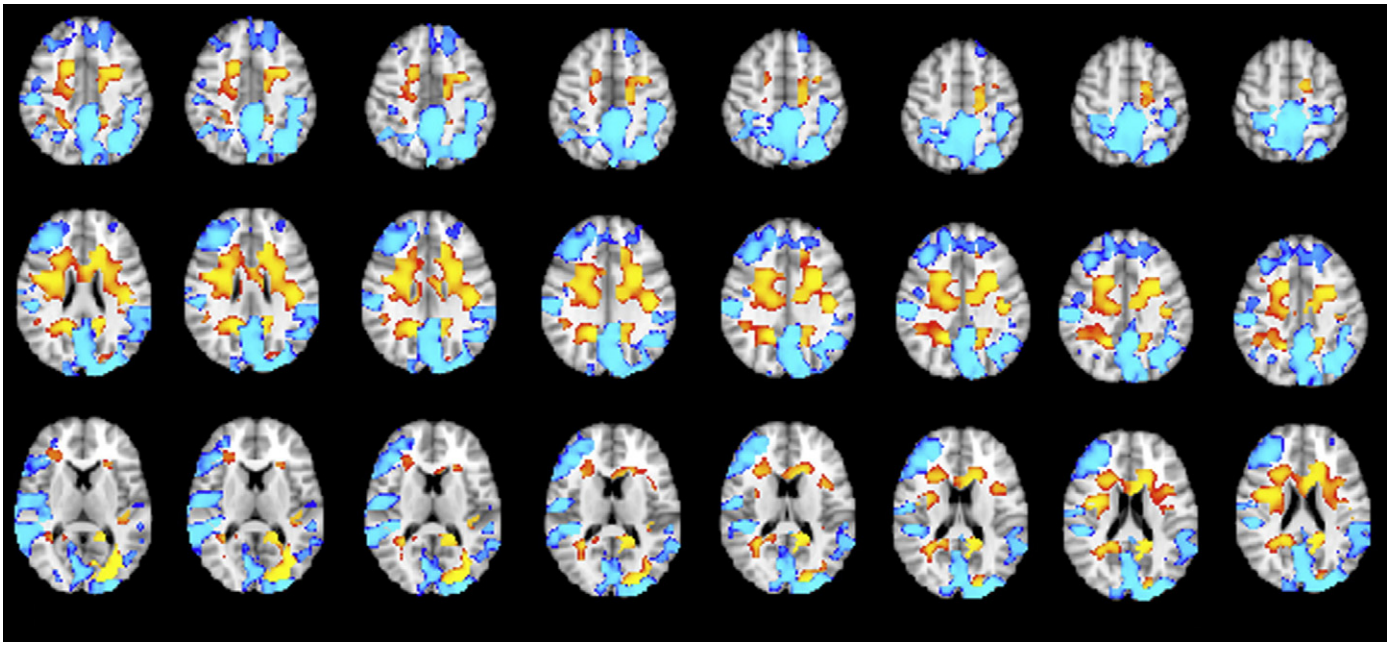

Fig. 2. Regions of grey (in blue–light blue) and white (in red–yellow) matter where volume shows significant (corrected $p<0.05$) decreases and increases, respectively, with age over time. See Results for details. Background image is the MNI152. Images are shown in radiological convention.

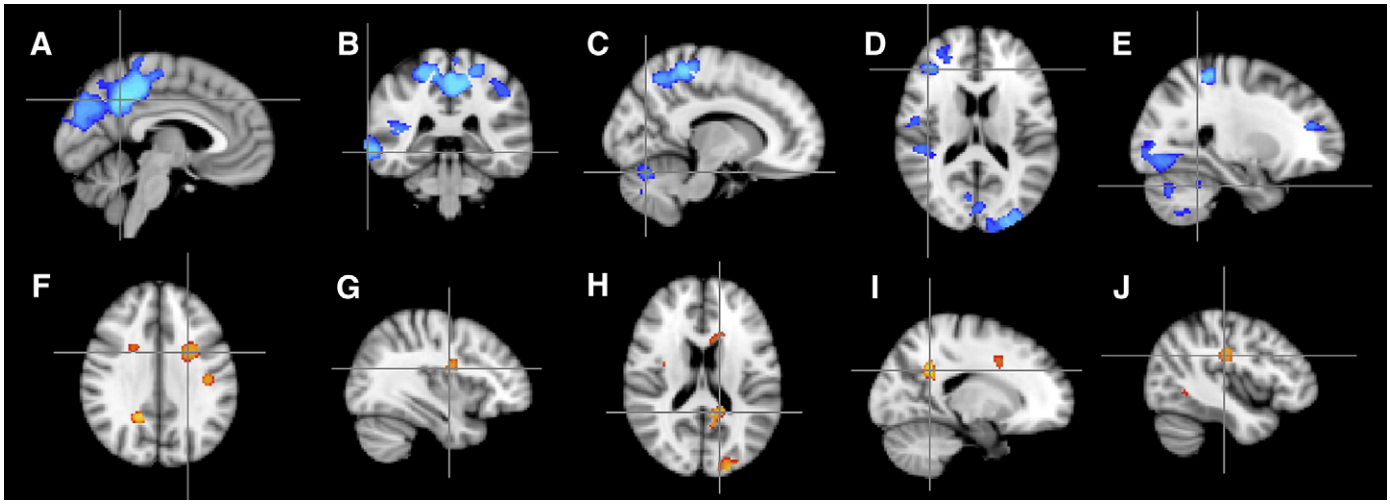

Fig. 3. Most significant regions of grey and white matter change. Blue–light blue and red–yellow represent the regions of grey and white matter where volume shows highly significant (corrected $p<0.005$) decreases and increases, respectively, with age over time in our group of adolescents. The crosshairs point to the local maxima in the (A) medial parietal (precuneus) cortex, (B) right posterior middle temporal gyrus, (C and E) right cerebellum, (D) right middle frontal gyrus, (F) left superior corona radiata, (G) right arcuate fasciculus, (H) splenium of the corpus callosum, (I) cingulum, and (L) left arcuate fasciculus. In panel L, part of the cluster in the left inferior longitudinal fasciculus is also visible. Background image is the MNI152. Images are shown in radiological convention.

No significant decreases in WM volume from baseline to follow-up were found and, as with the GM changes, there was no significant voxel-wise difference between males and females in these age-related WM volume changes.

Correlations between changes in voxel-wise FA and age over time: tract-based spatial statistics (TBSS)

Significant (corrected $p<0.05$) age-related increases in FA were found bilaterally in five WM clusters (Fig. 4). Four smaller clusters were located in the right hemisphere at the level of the forceps minor (two clusters), cingulum, and superior corona radiata (SCR). One cluster encompassed most of the remaining WM skeleton. The voxels surviving a higher p-value correction ($p<0.01$) were located in the right posterior corona radiata (PCR), including the right AF, and in the bilateral CST in a region spanning from the internal capsule (IC) to cerebral peduncle (CP) (Fig. 5 and Table 3).

Excluding the three left-handed subjects did not change the pattern of results (data not shown).

There were no significant decreases in FA from baseline to follow-up.

To test whether the increase in FA seen between baseline and follow-up scans was due to an increase in the parallel diffusivity or to a decrease in the perpendicular one, we estimated these diffusivities separately in averages across each cluster. Across all

Table 1
Local maxima within each significant cluster showing significant (corrected $p<0.005$) decrease in grey matter volume over time in adolescents.

Region (number of voxels)	Side	MNI			*t*-Statistic
		X	*Y*	*Z*	
Right middle frontal gyrus cluster (532)					
Frontal pole	R	28	40	18	5.78
Middle frontal gyrus	R	42	34	16	6.60
	R	36	28	30	5.89
Right parietotemporal cluster (2587)					
Superior temporal gyrus (middle)	R	52	−10	−8	5.77
Heschl's gyrus (medial)	R	44	−22	0	6.17
Supramarginal gyrus (anterior)	R	56	−24	32	5.93
Planum temporale	R	46	−34	10	5.09
	R	42	−36	10	5.37
Middle temporal gyrus (posterior)	R	70	−36	−8	6.17
Right anterior cerebellum cluster (11)	R	26	−48	−30	5.30
Parietal cluster (7364)					
Postcentral gyrus (superior)	L	−20	−38	58	4.37
Postcentral gyrus (superior)	R	14	−40	58	5.41
Medial parietal (precuneus) cortex	R	8	−42	56	5.48
Superior parietal lobule	R	26	−42	56	5.02
Medial parietal (precuneus) cortex	L	−4	−52	38	6.59
	L	−2	−56	34	5.58
Right cerebellar and occipital cluster (1722)					
Superior posterior cerebellum	R	12	−70	−22	6.11
Occipital fusiform gyrus	R	34	−70	−10	4.97
Superior posterior cerebellum	R	18	−76	−26	5.35
Posterior cerebellar lobe	R	20	−76	−40	4.94
Occipital fusiform gyrus	R	24	−78	−10	5.53
Occipital pole	R	26	−90	−6	4.45

Secondary local maxima are also shown when present. The grey matter clusters are ordered by decreasing *Y* coordinates of their primary local maxima.

Table 2
Local maxima within each significant cluster (corrected $p<0.005$) showing increased white matter volume over time in adolescents.

Region (number of voxels)	Side	MNI			*t*-Statistic
		X	*Y*	*Z*	
Left frontal white matter cluster (515)					
Superior corona radiata	L	−24	4	32	5.42
Body of the corpus callosum	L	−8	14	22	4.87
	L	−12	16	20	4.96
Right cingulum cluster (173)	R	18	−52	30	7.71
Left arcuate fasciculus cluster (133)	L	−42	−22	28	5.93
Right frontal white matter cluster (364)					
Superior corona radiata	R	22	8	34	4.87
	R	22	8	30	4.48
Arcuate fasciculus	R	46	0	24	4.86
	R	36	−6	20	4.95
Posterior callosum cluster (264)					
Splenium of the corpus callosum	L	−14	−46	18	5.66
Forceps major	L	−22	−50	6	5.55
	L	−16	−48	6	4.42
Left retrosplenial cluster (2077)					
Inferior longitudinal fasciculus	L	−34	−74	8	5.78
	L	−34	−86	−8	5.14
	L	−38	−60	−8	3.94
	L	−8	−82	−12	4.81

Secondary local maxima are also shown when present. The white matter clusters are ordered by decreasing *Z* coordinates of their primary local maxima.

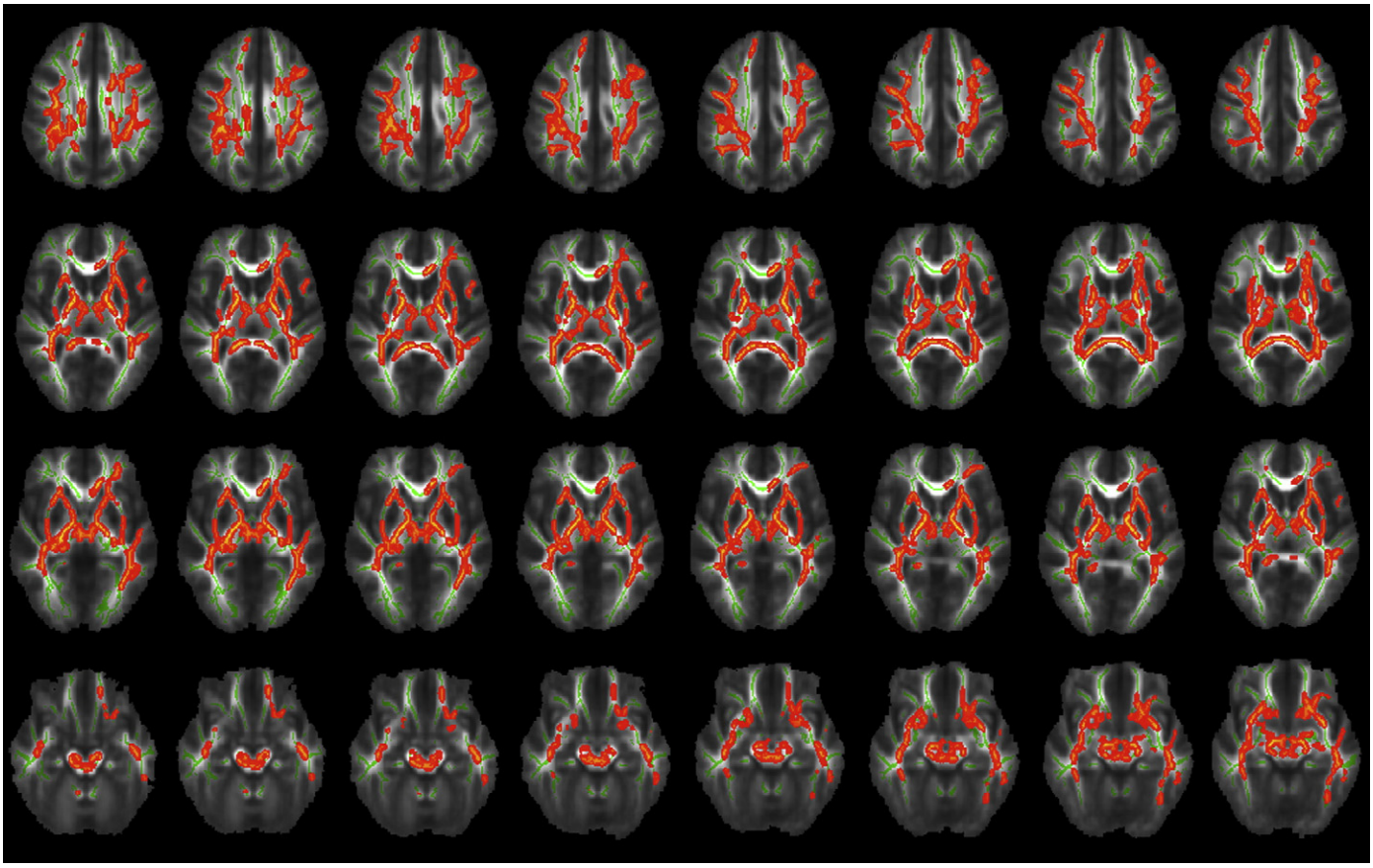

Fig. 4. White matter tracts (in red–yellow) showing significant (corrected $p<0.05$) age-related FA increases over time in our group of adolescents. See Results for details. Significant clusters are thickened for better visibility. Background image is the mean FA of all subjects, green is the white matter skeleton thresholded at FA>0.2 (visible where the age correlation did not reach significance). Images are shown in radiological convention.

significant clusters (Fig. 6) and for each cluster separately (data not shown), this analysis revealed a prevalent increase in parallel diffusivity with age, whereas perpendicular diffusivity remained relatively unchanged.

Relationships between FA, volume, and age: tractography analysis of the arcuate fasciculus and corticospinal tract

Pathways in both left and right AF and CST were traced in individual subjects. Pathways were incompletely traced in two (AF) and three (CST) subjects at baseline; therefore, they were discarded from the statistical analysis testing the effect of time (baseline versus follow-up) and hemisphere on changes in FA and volume in AF and CST (Table 4).

For the remaining subjects, an ANOVA on FA values within the AF revealed a significant main effect of time ($F_{1,21}=26.95$, $p<0.001$) due to significantly higher FA values in both left and right AF at follow-up ($t_{21}=4.29$, $p<0.001$; $t_{21}=4.01$ $p=0.001$, respectively). We also found a main effect of hemisphere ($F_{1,21}=25.82$, $p<0.001$) with higher FA values in the right than the left hemisphere at baseline ($t_{21}=4.97$, $p<0.001$) and at follow-up ($t_{21}=3.81$, $p=0.001$). No significant effects of time and hemisphere were found for FA values in the CST. There were no significant main effects or interactions in a similar ANOVA of the volumes of the AF and CST.

The same pattern of results was found after controlling the above analyses for the interscan interval.

FA and tract volume were not significantly correlated in any tracts at either time point.

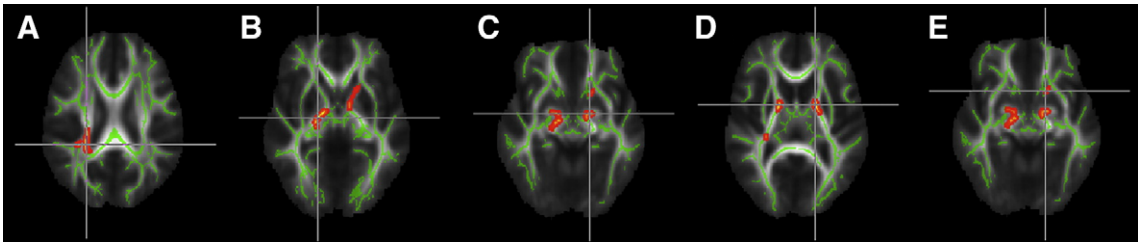

Fig. 5. Red–yellow shows the white matter tracts with highly significant (corrected $p<0.01$) age-related FA increases over time in our group of adolescents. The crosshairs point to the local maxima in the (A) right posterior corona radiata, (B) right posterior limb of the internal capsule, (C) left cerebral peduncle, (D) left anterior limb of the internal capsule, and (E) left anterior thalamic radiations. In panel A, part of the cluster in the right arcuate fasciculus is also visible. Significant clusters are thickened for better visibility. Background image is the mean FA of all subjects, green is the white matter skeleton thresholded at FA>0.2. Images are shown in radiological convention.

Table 3
Local maxima within each significant cluster (corrected $p<0.01$) showing increased white matter FA over time in adolescents.

Region (number of voxels)	Side	MNI			*t*-Statistic
		X	*Y*	*Z*	
Right posterior corona radiata cluster (548)	R	23	−38	31	3.96
	R	23	−38	27	3.67
	R	26	−39	23	5.00
	R	27	−44	23	4.08
	R	27	−41	22	3.91
	R	27	−35	21	3.69
Left internal capsule cluster (86)					
Posterior limb	L	−20	−6	13	3.83
	L	−17	−4	12	5.92
Anterior limb	L	−20	−8	11	3.24
	L	−16	−1	11	5.63
Posterior limb	L	−16	2	10	4.69
	L	−12	−3	6	2.82
Right internal capsule cluster (367)					
Posterior limb	R	18	−3	11	4.11
Anterior limb	R	12	0	4	3.06
Posterior limb	R	14	−7	1	3.21
Anterior limb	R	19	−13	0	4.14
Posterior limb	R	15	−11	−3	3.64
	R	13	−9	−4	3.78
Left cerebral peduncle cluster (102)					
Cerebral peduncle	L	−15	−6	−7	7.33
Internal capsule (posterior limb)	L	−12	−9	−7	3.86
Anterior thalamic radiations cluster (72)					
	L	−15	13	−7	2.93
	L	−13	3	−5	2.97
	L	−14	7	−4	2.67

Secondary local maxima are also shown when present. The white matter clusters are ordered by decreasing *Z* coordinates of their primary local maxima.

Discussion

We scanned 24 adolescents aged between 13.5 and 18.8 years and rescanned, on average, 2.5 years later. We found evidence for decreased grey and increased white matter volumes across many different brain regions. Furthermore, we found that FA, which reflects white matter microstructure, increased during the observation period in many fiber tracts mainly due to an increase in diffusivity along the main axis of these tracts. We discuss below each of these patterns of change, their inter-relationships, and speculate about the putative mechanisms underlying these changes.

Grey matter volume decreases

Grey matter volume changes in adolescence are dynamic. Previous studies have shown substantial reductions in the frontal, parietal, and temporo-occipital lobes (Gogtay et al., 2004; Sowell et al., 1999; Sowell et al., 2001). This loss continues during the transition from adolescence to young adulthood, especially in the dorsolateral prefrontal cortex (Giorgio et al., 2008; Sowell et al., 1999; Sowell et al., 2001). Specific processes underlying this reduction in grey matter have not been defined (Paus, 2005; Toga et al., 2006). Two mechanisms have been proposed: (1) an increase in the degree of myelination of intracortical axons (Nielsen, 1963; Yakovlev and Lecours, 1967) leading to an apparent loss of cortical grey matter as revealed by computational analyses of T1-weighted images and (2) a decreased number of synapses and complexity of axon ramifications due to accelerated elimination ("synaptic pruning"). Evidence for the latter has been demonstrated in primary visual (calcarine sulcus), auditory (Heschl's gyrus), and prefrontal cortex (middle frontal gyrus) (Huttenlocher, 1979; Huttenlocher and Dabholkar, 1997) and associated with increasing "fine-tuning" of neuronal connectivity (Cowan et al., 1984).

A large longitudinal cohort study (Giedd et al, 1999; Giedd 2004) has shown that the grey matter volume changes follow a complex

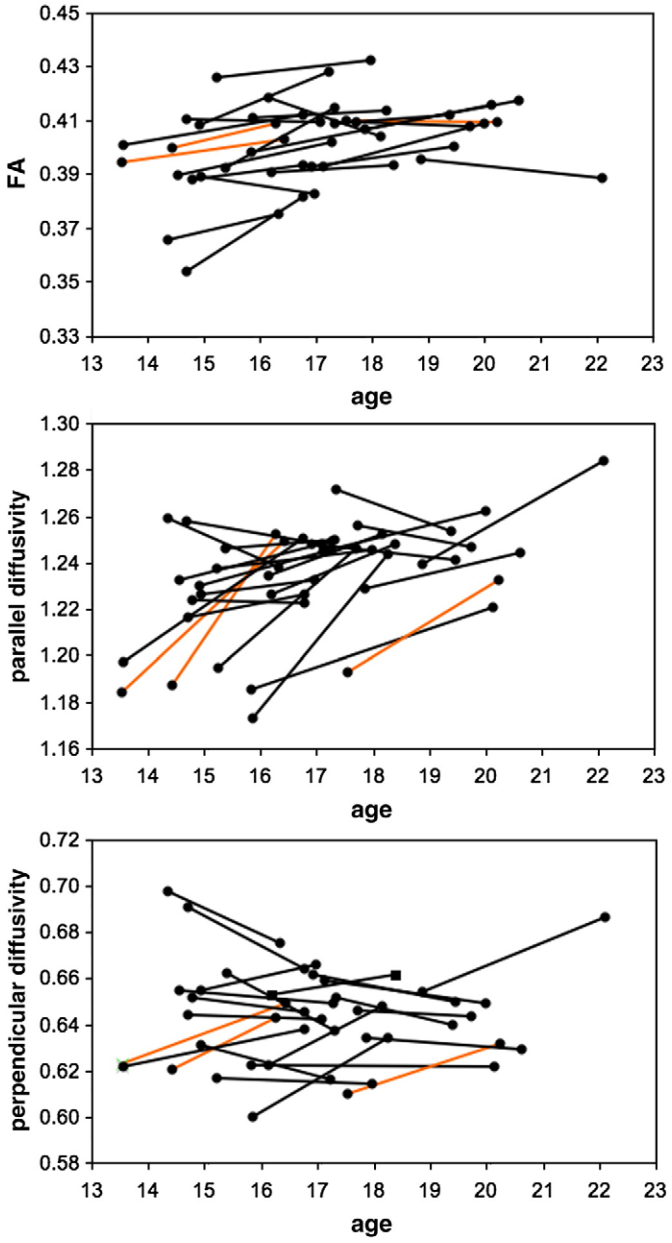

Fig. 6. Scatterplots, with longitudinal data points connected by a line, of mean values of FA, parallel and perpendicular diffusivity from white matter regions showing significant relationship with age over time in adolescents. Orange lines indicate the three left-handed subjects. Values of diffusivities are expressed in $\times 10^{-3}$ mm^2/s.

Table 4
Mean and standard deviation of FA and volume values in left and right arcuate fasciculus (AF) and corticospinal tract (CST) at baseline (time 1) and end of follow-up (time 2).

Tract	Side	Measures	Time 1	Time 2	Significance
AF	L	FA	0.404 ± 0.020	0.417 ± 0.015	$p<0.001$
		Volume (ml)	5.451 ± 0.785	5.490 ± 0.616	NS
	R	FA	0.419 ± 0.021	0.429 ± 0.017	$p<0.001$
		Volume (ml)	4.735 ± 0.729	4.876 ± 0.648	NS
CST	L	FA	0.439 ± 0.020	0.449 ± 0.021	NS
		Volume (ml)	18.897 ± 2.028	18.078 ± 1.883	NS
	R	FA	0.441 ± 0.025	0.449 ± 0.020	NS
		Volume (ml)	19.290 ± 2.181	18.701 ± 2.332	NS

pattern of maturation during childhood and adolescence and that the peak of change is different for males and females across brain lobes. In our study, we saw a linear decrease in grey matter volume across different parts of the cerebral cortex. The relatively small number and restricted age range of our adolescent subjects precluded detailed statistical analysis, although it appears that our findings relate to the latter half of growth curves normally observed during childhood and adolescence (Giedd, 2004; Giedd et al., 1999).

Another larger longitudinal study of children and adolescents has reported that different cortical grey matter regions follow different developmental trajectories: these appear simple and linear in limbic areas but are potentially more complex in the higher order association regions (Shaw et al., 2008). It has been suggested that there is a distinct developmental sequence of cortical grey matter loss, with primary areas maturing earlier and higher order association areas following later (Gogtay et al., 2004; Shaw et al., 2008). However, while we saw a decrease in grey matter volume over time in higher order association areas such as the dorsolateral prefrontal cortex and the superior temporal gyrus, generally consistent with this notion, we also found grey matter changes in primary sensorimotor cortex (precentral and postcentral gyri) and primary sensory cortex (calcarine sulcus), suggesting that development in these areas also continues during late adolescence.

White matter volume increases

In contrast to the complex pattern of development of grey matter, it is clear from conventional structural MRI studies (Courchesne et al., 2000; Paus et al., 1999; Pfefferbaum et al., 1994) that white matter volume increases steadily throughout adolescence and adulthood. Only slight differences in the trajectory for white matter maturation have been reported between the four major lobes of the brain (Giedd, 2004; Giedd et al., 1999; Perrin et al., 2008). An increase in white matter density and volume has been reported in previous cross-sectional studies on children and adolescents at the level of the corticospinal tract (Barnea-Goraly et al., 2005; Paus et al., 1999), interthalamic pathways (Barnea-Goraly et al., 2005), corpus callosum (Barnea-Goraly et al., 2005), and arcuate fasciculus (Barnea-Goraly et al., 2005; Paus et al., 1999).

In the current study, we found age-related increase in white matter volumes over adolescence in several regions. These included regions of the frontal lobe, in which a significant increase in white matter density and volume has been previously reported in cross-sectional studies on children and adolescents aged 5–19 years (Barnea-Goraly et al., 2005; Reiss et al., 1996). We also found a significant association between increased white matter volume and age in the corpus callosum, particularly at the level of the body and the splenium. These findings are in agreement with those of previous longitudinal volumetric studies in which maturation changes were described as following a rostrocaudal direction, with the anterior sections maturing earlier in childhood and more caudal regions maturing later (Giedd, 2004; Thompson et al., 2000). In our adolescent cohort, we also found an increase of white matter volume in the arcuate fasciculus bilaterally but not in the internal capsule (but see below for analysis of FA). The earlier study by Paus et al. (1999) described changes in white matter volume in these two white matter regions in a large cross-sectional cohort ranging in age from early childhood to late adolescence. A likely explanation for this discrepancy is the narrow age range for subjects in our study, which focused on the late adolescent period.

FA increases and tractography analysis

In addition to increases in white matter volume, we also found age-related increases in FA in several white matter tracts. This accords with the findings from a number of cross-sectional studies in adolescence of increasing FA with age in: anterior limb of the internal capsule (Bonekamp et al., 2006; Schmithorst et al., 2002; Snook et al., 2005); superior longitudinal fasciculus (Bonekamp et al., 2006; Lebel et al., 2008); left and right arcuate fasciculus (Ashtari et al., 2007; Bonekamp et al., 2006; Eluvathingal et al., 2007; Schmithorst et al., 2002); corticospinal tract (Eluvathingal et al., 2007; Giorgio et al., 2008; Lebel et al., 2008; Schmithorst et al., 2002; Snook et al., 2005); left and right inferior fronto-occipital/inferior longitudinal fasciculus (Eluvathingal et al., 2007; Lebel et al., 2008; Schmithorst et al., 2002); genu, splenium, and body of the corpus callosum (Ashtari et al., 2007; Barnea-Goraly et al., 2005; Giorgio et al., 2008; Muetzel et al., 2008; Snook et al., 2005); and cingulum (Bonekamp et al., 2006; Lebel et al., 2008).

We thus have confirmed and extended our earlier cross-sectional DTI study in adolescence (Giorgio et al., 2008). While some differences are apparent between the two studies (e.g., in the number of regions showing increases in FA over time and in their hemispheric location), these are simply due, we believe, to the greater sensitivity of having a paired longitudinal design and of an improved approach to statistical thresholding. For example, the significant correlation between FA in many parts of the corticospinal tract and age over time found here with voxel-wise analysis of the white matter skeleton is consistent with our earlier study, in which a correlation between FA and age was found in a region adjacent to the body of the corpus callosum in the right hemisphere and in the right superior corona radiata, which includes fibers projecting to and from the cerebral cortex and descending motor fibers contributing to the corticospinal tract. Overall, these findings fit with the concept of refinement of capacity for improved motor skills during adolescence (Forssberg et al., 1991; Lawrence and Hopkins, 1976; Muetzel et al., 2008).

Interestingly, our tractography analysis of the corticospinal tract did not reveal evidence for significant increasing FA averaged across the entire tract between the two time points. However, we found a developmental FA increase in specific regions within the anterior and posterior limbs of the internal capsule, extending the findings from previous studies, where such an increase was demonstrated only in the anterior limb (Bonekamp et al., 2006; Schmithorst et al., 2002; Snook et al., 2005). These changes must reflect maturation of distinct, specific pathways. The anterior limb of the internal capsule mainly contains thalamocortical fibers connecting nuclei of the thalamus to the frontal lobes. The posterior limb of the internal capsule mainly contains fibers belonging to the corticospinal tracts.

We also found a significant increase of FA in the different parts of the superior longitudinal fasciculus, including the arcuate fasciculus bilaterally. This was confirmed by both the voxel-wise analysis of the white matter skeleton and by the comparison of FA values in the whole tractography-derived tract between the two time points. The arcuate fasciculus has been previously segmented in humans using a streamline tractography approach (Makris et al., 2005) based on a priori knowledge from primates. The arcuate fasciculus is the fourth subdivision of the superior longitudinal fasciculus, originating from the caudal part of the superior temporal gyrus, arching around the caudal end of the Sylvian fissure and extending to the lateral prefrontal cortex (Frey et al., 2008). It is a functionally relevant white matter pathway that, together with other fibers in the superior longitudinal fasciculus, provides a connection between anterior (Broca's) and posterior (Wernicke's) speech regions in the human brain (Benson et al., 1973; Geschwind, 1970; Wernicke, 1968). In our study, FA values computed from the whole arcuate fasciculus obtained by tractography were significantly higher on the right compared to the left hemisphere at both time points. This was not explained by differences in segmented tract volumes and appears to conflict with previous cross-sectional brain asymmetry DTI studies in both children and adolescents (Eluvathingal et al., 2007) and adult subjects (Buchel et al., 2004), in which a voxel-wise leftward FA asymmetry (left>right) in the frontotemporal segment of the arcuate fasciculus was found, consistent with the lateralization of language to

the dominant hemisphere. The differences may reflect different biases in localization of changes. In both the aforementioned studies (Buchel et al., 2004; Eluvathingal et al., 2007), a rightward FA asymmetry (right>left) was found in the frontoparietal segment of the arcuate fasciculus.

Recent MRI studies suggest that the development of the brain may be sexually dimorphic during adolescence (Lenroot and Giedd, 2006; Schmithorst et al., 2008). This may also apply to white matter microstructure. For example, greater FA values have been demonstrated in a large group of children and adolescents in associative white matter areas (including the frontal lobes) in boys and in the splenium of the corpus callosum in girls (Schmithorst et al., 2008). The lack of significant sex differences or significant interactions between sex and age over adolescence found here is in agreement with some previous studies (Bonekamp et al., 2006; Eluvathingal et al., 2007; Giorgio et al., 2008). However, our sample size of 24 subjects was underpowered to detect differences between the smaller subgroups of males and females.

Assessment of parallel and perpendicular diffusivity in addition to FA should add further insight into mechanisms underlying these FA changes. However, findings in previous developmental studies have been inconsistent, with varying patterns of diffusivity changes explaining age-related FA increases in the white matter (Ashtari et al., 2007; Bonekamp et al., 2006; Eluvathingal et al., 2007; Giorgio et al., 2008; Lebel et al., 2008). The FA increases reported in our study were driven primarily by increased parallel diffusivity over time with relatively no changes in the perpendicular diffusivity. This is in line with the results of a previous cross-sectional DTI study in later adolescence (Ashtari et al., 2007).

The anatomical interpretation of this pattern of an increase in FA, which certainly cannot be considered as a specific marker of myelination (Beaulieu and Allen, 1994), is not certain, but it likely reflects (1) increased axonal fiber diameter, which has been related to the increase in height with age (Eyre et al., 1991); or (2) the presence of more straightened fibers, due to their reduced tortuosity, as shown in electron microscopy studies of the central and peripheral nervous systems in developing rats (Joosten and Bar, 1999; Takahashi et al., 2000) and across a wide range of animal species (Dodd and Jessell, 1988); or (3) some combination of (1) and (2).

Whereas the exact anatomical interpretation of increasing FA with age is not entirely clear, there is growing evidence for its importance as behavioral correlates are defined. For example, maturation of the white matter, as indicated by higher FA, is associated with full-scale IQ scores (Schmithorst et al., 2005), working memory capacity, and reading ability (Nagy et al., 2004) and with language-related cognitive tests in adolescent males (Ashtari et al., 2007).

Relationship between grey matter, white matter, and FA changes

Using a longitudinal design, we were able to map changes in grey and white matter volumes and white matter FA and some of their inter-relationships. The close spatial relationship between changes in grey matter volume of the frontoparietal lobe and adjacent white matter FA is consistent with a study in children and adolescents aged 8–18 years in which a combined DTI and functional MRI (FMRI) analysis revealed a joint maturation of these two areas as part of a functional network underlying working memory (Olesen et al., 2003). In the current study, we also found a decrease of grey matter volume in the dorsolateral prefrontal cortex. This is the structure to mature last in the frontal lobe, showing a reduction in grey matter only at the end of adolescence (Gogtay et al., 2004). The fact that this coincides with its later myelination (Jernigan and Tallal, 1990; Yakovlev and Lecours, 1967) suggests that myelination and synaptic pruning, at least in this region, may occur in parallel (Gogtay et al., 2004).

We also found both FA and volume changes in the white matter bilaterally. Overlaps between age-related FA and white matter volume increases were present at the level of the bilateral superior corona radiata, bilateral superior longitudinal fasciculus (including arcuate fasciculus), bilateral cingulum, left part of the genu of the corpus callosum, bilateral body of the corpus callosum, splenium of the corpus callosum, bilateral forceps major, left uncinate fasciculus, and bilateral inferior fronto-occipital/longitudinal fasciculus. Our findings differ from those of a cross-sectional study of children and adolescents aged 6–19 years, where the most significant overlaps between increased FA and white matter volume were observed in the internal capsule and in regions corresponding to white matter pathways within the thalamus (Barnea-Goraly et al., 2005). The reason for this disparity between FA and white matter volume changes may reflect the existence of true histological differences during the development of the white matter or indeed the differing power of the two methods used to discriminate white matter changes.

It has often been assumed that the increase in myelination during development that is documented in histological studies (Benes, 1989; Benes et al., 1994; Yakovlev and Lecours, 1967) is the principal factor determining an increase in white matter volume. This view is perhaps too simplistic. Other factors, such as an increase of the fiber diameter, also may contribute (Paus et al., 2008). In fact, a recent study on adolescents found significant relationships between age-related increases in white matter volume and decreases in magnetization transfer ratio (MTR), a putative marker of myelin content in the white matter (Perrin et al., 2008). The idea of an increased fiber diameter during adolescence is supported in our study by the fact that increases in FA were mainly driven by increases in parallel diffusivity. This mechanism would explain the age-related changes that we found in many fiber tracts, at least in those showing overlaps between FA and white matter volume increase.

A limitation of our study is the relatively small number of subjects involved, which precludes analyses of the effects of gender and handedness. However, a larger study including cognitive measures is planned. A recent meta-analysis (Hasan et al., 2007) has shown that the findings of grey and white matter changes in this age range are heavily influenced by the varying MRI techniques and analyses used. One of the strengths of this study, therefore, lies in the use of imaging analysis with proven sensitivity and reproducibility (Good et al., 2001; Smith et al., 2006), alongside quality control of the scanning procedures and image acquisition.

References

Andersson, J.L.R., Jenkinson, M., Smith, S., 2007a. Non-linear optimisation. FMRIB technical report TR07JA1 from www.fmrib.ox.ac.uk/analysis/techrep.

Andersson, J.L.R., Jenkinson, M., Smith, S., 2007b. Non-linear registration, aka spatial normalisation. FMRIB technical report TR07JA2 from www.fmrib.ox.ac.uk/analysis/techrep.

Ashtari, M., Cervellione, K.L., Hasan, K.M., Wu, J., McIlree, C., Kester, H., Ardekani, B.A., Roofeh, D., Szeszko, P.R., Kumra, S., 2007. White matter development during late adolescence in healthy males: a cross-sectional diffusion tensor imaging study. NeuroImage.

Barnea-Goraly, N., Menon, V., Eckert, M., Tamm, L., Bammer, R., Karchemskiy, A., Dant, C.C., Reiss, A.L., 2005. White matter development during childhood and adolescence: a cross-sectional diffusion tensor imaging study. Cereb. Cortex 15, 1848–1854.

Beaulieu, C., Allen, P.S., 1994. Determinants of anisotropic water diffusion in nerves. Magn. Reson. Med. 31, 394–400.

Behrens, T.E., Johansen-Berg, H., Woolrich, M.W., Smith, S.M., Wheeler-Kingshott, C.A., Boulby, P.A., Barker, G.J., Sillery, E.L., Sheehan, K., Ciccarelli, O., Thompson, A.J., Brady, J.M., Matthews, P.M., 2003. Non-invasive mapping of connections between human thalamus and cortex using diffusion imaging. Nat. Neurosci. 6, 750–757.

Benes, F.M., 1989. Myelination of cortical–hippocampal relays during late adolescence. Schizophr. Bull. 15, 585–593.

Benes, F.M., Turtle, M., Khan, Y., Farol, P., 1994. Myelination of a key relay zone in the hippocampal formation occurs in the human brain during childhood, adolescence, and adulthood. Arch. Gen. Psychiatry 51, 477–484.

Benson, D.F., Sheremata, W.A., Bouchard, R., Segarra, J.M., Price, D., Geschwind, N., 1973. Conduction aphasia. A clinicopathological study. Arch. Neurol. 28, 339–346.

Bhagat, Y.A., Beaulieu, C., 2004. Diffusion anisotropy in subcortical white matter and cortical gray matter: changes with aging and the role of CSF-suppression. J. Magn. Reson. Imaging 20, 216–227.

Bonekamp, D., Nagae, L.M., Degaonkar, M., Matson, M., Abdalla, W.M., Barker, P.B., Mori, S., Horska, A., 2006. Diffusion tensor imaging in children and adolescents: reproducibility, hemispheric, and age-related differences. NeuroImage.
Buchel, C., Raedler, T., Sommer, M., Sach, M., Weiller, C., Koch, M.A., 2004. White matter asymmetry in the human brain: a diffusion tensor MRI study. Cereb. Cortex 14, 945–951.
Courchesne, E., Chisum, H.J., Townsend, J., Cowles, A., Covington, J., Egaas, B., Harwood, M., Hinds, S., Press, G.A., 2000. Normal brain development and aging: quantitative analysis at in vivo MR imaging in healthy volunteers. Radiology 216, 672–682.
Cowan, W.M., Fawcett, J.W., O'Leary, D.D., Stanfield, B.B., 1984. Regressive events in neurogenesis. Science 225, 1258–1265.
Dodd, J., Jessell, T.M., 1988. Axon guidance and the patterning of neuronal projections in vertebrates. Science 242, 692–699.
Eluvathingal, T.J., Hasan, K.M., Kramer, L., Fletcher, J.M., Ewing-Cobbs, L., 2007. Quantitative diffusion tensor tractography of association and projection fibers in normally developing children and adolescents. Cereb. Cortex 17, 2760–2768.
Eyre, J.A., Miller, S., Ramesh, V., 1991. Constancy of central conduction delays during development in man: investigation of motor and somatosensory pathways. J. Physiol. 434, 441–452.
Forssberg, H., Eliasson, A.C., Kinoshita, H., Johansson, R.S., Westling, G., 1991. Development of human precision grip. I: basic coordination of force. Exp. Brain Res. 85, 451–457.
Frey, S., Campbell, J.S., Pike, G.B., Petrides, M., 2008. Dissociating the human language pathways with high angular resolution diffusion fiber tractography. J. Neurosci. 28, 11435–11444.
Geschwind, N., 1970. The organization of language and the brain. Science 170, 940–944.
Giedd, J.N., 2004. Structural magnetic resonance imaging of the adolescent brain. Ann. N. Y. Acad. Sci. 1021, 77–85.
Giedd, J.N., Blumenthal, J., Jeffries, N.O., Castellanos, F.X., Liu, H., Zijdenbos, A., Paus, T., Evans, A.C., Rapoport, J.L., 1999. Brain development during childhood and adolescence: a longitudinal MRI study. Nat. Neurosci. 2, 861–863.
Giorgio, A., Watkins, K.E., Douaud, G., James, A.C., James, S., De Stefano, N., Matthews, P.M., Smith, S.M., Johansen-Berg, H., 2008. Changes in white matter microstructure during adolescence. NeuroImage 39, 52–61.
Gogtay, N., Giedd, J.N., Lusk, L., Hayashi, K.M., Greenstein, D., Vaituzis, A.C., Nugent 3rd, T.F., Herman, D.H., Clasen, L.S., Toga, A.W., Rapoport, J.L., Thompson, P.M., 2004. Dynamic mapping of human cortical development during childhood through early adulthood. Proc. Natl. Acad. Sci. U. S. A. 101, 8174–8179.
Good, C.D., Johnsrude, I.S., Ashburner, J., Henson, R.N., Friston, K.J., Frackowiak, R.S., 2001. A voxel-based morphometric study of ageing in 465 normal adult human brains. NeuroImage 14, 21–36.
Hasan, K.M., Halphen, C., Sankar, A., Eluvathingal, T.J., Kramer, L., Stuebing, K.K., Ewing-Cobbs, L., Fletcher, J.M., 2007. Diffusion tensor imaging-based tissue segmentation: validation and application to the developing child and adolescent brain. NeuroImage 34, 1497–1505.
Huttenlocher, P.R., 1979. Synaptic density in human frontal cortex—developmental changes and effects of aging. Brain. Res. 163, 195–205.
Huttenlocher, P.R., Dabholkar, A.S., 1997. Regional differences in synaptogenesis in human cerebral cortex. J. Comp. Neurol. 387, 167–178.
Jenkinson, M., Smith, S., 2001. A global optimisation method for robust affine registration of brain images. Med. Image. Anal. 5, 143–156.
Jernigan, T.L., Tallal, P., 1990. Late childhood changes in brain morphology observable with MRI. Dev. Med. Child. Neurol. 32, 379–385.
Joosten, E.A., Bar, D.P., 1999. Axon guidance of outgrowing corticospinal fibres in the rat. J. Anat. 194 (Pt. 1), 15–32.
Lawrence, D.G., Hopkins, D.A., 1976. The development of motor control in the rhesus monkey: evidence concerning the role of corticomotoneuronal connections. Brain 99, 235–254.
Lebel, C., Walker, L., Leemans, A., Phillips, L., Beaulieu, C., 2008. Microstructural maturation of the human brain from childhood to adulthood. NeuroImage 40, 1044–1055.
Lenroot, R.K., Giedd, J.N., 2006. Brain development in children and adolescents: insights from anatomical magnetic resonance imaging. Neurosci. Biobehav. Rev. 30, 718–729.
Makris, N., Kennedy, D.N., McInerney, S., Sorensen, A.G., Wang, R., Caviness Jr., V.S., Pandya, D.N., 2005. Segmentation of subcomponents within the superior longitudinal fascicle in humans: a quantitative, in vivo, DT-MRI study. Cereb. Cortex 15, 854–869.
Muetzel, R.L., Collins, P.F., Mueller, B.A., A, Schissel, A.M., Lim, K.O., Luciana, M., 2008. The development of corpus callosum microstructure and associations with bimanual task performance in healthy adolescents. NeuroImage 39 (4), 1918–1925.
Nagy, Z., Westerberg, H., Klingberg, T., 2004. Maturation of white matter is associated with the development of cognitive functions during childhood. J. Cogn. Neurosci. 16, 1227–1233.
Nichols, T.E., Holmes, A.P., 2002. Nonparametric permutation tests for functional neuroimaging: a primer with examples. Hum. Brain Mapp. 15, 1–25.
Nielsen, J.M., 1963. The myelogenetic studies of Paul Flechsig. Bull. Los Angel. Neuro. Soc. 28, 127–134.
Olesen, P.J., Nagy, Z., Westerberg, H., Klingberg, T., 2003. Combined analysis of DTI and fMRI data reveals a joint maturation of white and grey matter in a fronto-parietal network. Brain. Res. Cogn. Brain. Res. 18, 48–57.
Paus, T., 2005. Mapping brain maturation and cognitive development during adolescence. Trends Cogn. Sci. 9, 60–68.
Paus, T., Keshavan, M., Giedd, J.N., 2008. Why do many psychiatric disorders emerge during adolescence? Nat. Rev. Neurosci. 9, 947–957.
Paus, T., Zijdenbos, A., Worsley, K., Collins, D.L., Blumenthal, J., Giedd, J.N., Rapoport, J.L., Evans, A.C., 1999. Structural maturation of neural pathways in children and adolescents: in vivo study. Science 283, 1908–1911.
Perrin, J.S., Herve, P.Y., Leonard, G., Perron, M., Pike, G.B., Pitiot, A., Richer, L., Veillette, S., Pausova, Z., Paus, T., 2008. Growth of white matter in the adolescent brain: role of testosterone and androgen receptor. J. Neurosci. 28, 9519–9524.
Pfefferbaum, A., Mathalon, D.H., Sullivan, E.V., Rawles, J.M., Zipursky, R.B., Lim, K.O., 1994. A quantitative magnetic resonance imaging study of changes in brain morphology from infancy to late adulthood. Arch. Neurol. 51, 874–887.
Reiss, A.L., Abrams, M.T., Singer, H.S., Ross, J.L., Denckla, M.B., 1996. Brain development, gender and IQ in children. A volumetric imaging study. Brain 119 (Pt. 5), 1763–1774.
Schmithorst, V.J., Wilke, M., Dardzinski, B.J., Holland, S.K., 2002. Correlation of white matter diffusivity and anisotropy with age during childhood and adolescence: a cross-sectional diffusion-tensor MR imaging study. Radiology 222, 212–218.
Schmithorst, V.J., Wilke, M., Dardzinski, B.J., Holland, S.K., 2005. Cognitive functions correlate with white matter architecture in a normal pediatric population: a diffusion tensor MRI study. Hum. Brain Mapp. 26, 139–147.
Schmithorst, V.J., Holland, S.K., Dardzinski, B.J., 2008. Developmental differences in white matter architecture between boys and girls. Hum. Brain Mapp. 29, 696–710.
Shaw, P., Kabani, N.J., Lerch, J.P., Eckstrand, K., Lenroot, R., Gogtay, N., Greenstein, D., Clasen, L., Evans, A., Rapoport, J.L., Giedd, J.N., Wise, S.P., 2008. Neurodevelopmental trajectories of the human cerebral cortex. J. Neurosci. 28, 3586–3594.
Smith, S.M., 2002. Fast robust automated brain extraction. Hum. Brain Mapp. 17, 143–155.
Smith, S.M., Jenkinson, M., Johansen-Berg, H., Rueckert, D., Nichols, T.E., Mackay, C.E., Watkins, K.E., Ciccarelli, O., Cader, M.Z., Matthews, P.M., Behrens, T.E., 2006. Tract-based spatial statistics: voxelwise analysis of multi-subject diffusion data. NeuroImage 31, 1487–1505.
Smith, S.M., Jenkinson, M., Woolrich, M.W., Beckmann, C.F., Behrens, T.E., Johansen-Berg, H., Bannister, P.R., De Luca, M., Drobnjak, I., Flitney, D.E., Niazy, R.K., Saunders, J., Vickers, J., Zhang, Y., De Stefano, N., Brady, J.M., Matthews, P.M., 2004. Advances in functional and structural MR image analysis and implementation as FSL. NeuroImage 23 (Suppl. 1), S208–S219.
Smith, S.M., Nichols, T.E., 2009. Threshold-free cluster enhancement: addressing problems of smoothing, threshold dependence and localisation in cluster inference. NeuroImage 44, 83–98.
Snook, L., Paulson, L.A., Roy, D., Phillips, L., Beaulieu, C., 2005. Diffusion tensor imaging of neurodevelopment in children and young adults. NeuroImage 26, 1164–1173.
Sowell, E.R., Thompson, P.M., Holmes, C.J., Jernigan, T.L., Toga, A.W., 1999. In vivo evidence for post-adolescent brain maturation in frontal and striatal regions. Nat. Neurosci. 2, 859–861.
Sowell, E.R., Thompson, P.M., Tessner, K.D., Toga, A.W., 2001. Mapping continued brain growth and gray matter density reduction in dorsal frontal cortex: inverse relationships during postadolescent brain maturation. J. Neurosci. 21, 8819–8829.
Spear, L.P., 2000. The adolescent brain and age-related behavioral manifestations. Neurosci. Biobehav. Rev. 24, 417–463.
Suzuki, Y., Matsuzawa, H., Kwee, I.L., Nakada, T., 2003. Absolute eigenvalue diffusion tensor analysis for human brain maturation. NMR Biomed. 16, 257–260.
Takahashi, M., Ono, J., Harada, K., Maeda, M., Hackney, D.B., 2000. Diffusional anisotropy in cranial nerves with maturation: quantitative evaluation with diffusion MR imaging in rats. Radiology 216, 881–885.
Thompson, P.M., Giedd, J.N., Woods, R.P., MacDonald, D., Evans, A.C., Toga, A.W., 2000. Growth patterns in the developing brain detected by using continuum mechanical tensor maps. Nature 404, 190–193.
Toga, A.W., Thompson, P.M., Sowell, E.R., 2006. Mapping brain maturation. Trends Neurosci. 29, 148–159.
Wakana, S., Jiang, H., Nagae-Poetscher, L.M., van Zijl, P.C., Mori, S., 2004. Fiber tract-based atlas of human white matter anatomy. Radiology 230, 77–87.
Wechsler, D., 1999. Wechsler Abbreviated Scale of Intelligence. The Psychological Corporation, New York.
Wernicke, C., 1968. The symptom complex of aphasia (1874). Reprinted in English in Proc. Boston Colloq. Philos. Sci. 4, 34–97.
Yakovlev, P.I., Lecours, A.R., 1967. The myelogenetic cycles of regional maturation of the brain. In: Minkowski, A. (Ed.), Regional development of the brain in early life. InBlackwell Scientific Publications, Oxford, pp. 3–70.
Zhang, Y., Brady, M., Smith, S., 2001. Segmentation of brain MR images through a hidden Markov random field model and the expectation-maximization algorithm. IEEE. Trans. Med. Imaging 20, 45–57.